Phys. Lett. B **403** (1997) 185
UMS/HEP/96-001
FERMILAB-Pub-96-206-E

Observation of $D-\pi$ Production Correlations in 500 GeV $\pi^- - N$ Interactions

E. M. Aitala,[8] S. Amato,[1] J. C. Anjos,[1] J. A. Appel,[5] D. Ashery,[14] S. Banerjee,[5] I. Bediaga,[1] G. Blaylock,[2] S. B. Bracker,[15] P. R. Burchat,[13] R. A. Burnstein,[6] T. Carter,[5] H. S. Carvalho,[1] N. K. Copty,[12] I. Costa,[1] L. M. Cremaldi,[8] C. Darling,[18] K. Denisenko,[5] A. Fernandez,[11] P. Gagnon,[2] S. Gerzon,[14] K. Gounder,[8] A. M. Halling,[5] G. Herrera,[4] G. Hurvits,[14] C. James,[5] P. A. Kasper,[6] S. Kwan,[5] D. C. Langs,[10] J. Leslie,[2] B. Lundberg,[5] S. MayTal-Beck,[14] B. T. Meadows,[3] J. R. T. de Mello Neto,[1] R. H. Milburn,[16] J. M. de Miranda,[1] A. Napier,[16] A. Nguyen,[7] A. B. d'Oliveira,[3,11] K. O'Shaughnessy,[2] K. C. Peng,[6] L. P. Perera,[3] M. V. Purohit,[12] B. Quinn,[8] S. Radeztsky,[17] A. Rafatian,[8] N. W. Reay,[7] J. J. Reidy,[8] A. C. dos Reis,[1] H. A. Rubin,[6] A. K. S. Santha,[3] A. F. S. Santoro,[1] A. J. Schwartz,[10] M. Sheaff,[17] R. A. Sidwell,[7] A. J. Slaughter,[18] M. D. Sokoloff,[3] N. R. Stanton,[7] K. Stenson,[17] D. J. Summers,[8] S. Takach,[18] K. Thorne,[5] A. K. Tripathi,[9] S. Watanabe,[17] R. Weiss-Babai,[14] J. Wiener,[10] N. Witchey,[7] E. Wolin,[18] D. Yi,[8] S. Yoshida,[7] R. Zaliznyak,[13] C. Zhang[7]

(Fermilab E791 Collaboration)

[1] *Centro Brasileiro de Pesquisas Físicas, Rio de Janeiro, Brazil*

[2] *University of California, Santa Cruz, California 95064*

[3] *University of Cincinnati, Cincinnati, Ohio 45221*

[4] *CINVESTAV, Mexico*

[5] *Fermilab, Batavia, Illinois 60510*

[6] *Illinois Institute of Technology, Chicago, Illinois 60616*

[7] *Kansas State University, Manhattan, Kansas 66506*

[8] *University of Mississippi, University, Mississippi 38677*

[9] *The Ohio State University, Columbus, Ohio 43210*

[10] *Princeton University, Princeton, New Jersey 08544*

[11] *Universidad Autonoma de Puebla, Mexico*

[12] *University of South Carolina, Columbia, South Carolina 29208*

[13] *Stanford University, Stanford, California 94305*

[14] *Tel Aviv University, Tel Aviv, Israel*

[15] *317 Belsize Drive, Toronto, Canada*

[16] *Tufts University, Medford, Massachusetts 02155*

[17] *University of Wisconsin, Madison, Wisconsin 53706*

[18] *Yale University, New Haven, Connecticut 06511*

(19 June 1997)

Abstract

We study the charge correlations between charm mesons produced in 500 GeV $\pi^- - N$ interactions and the charged pions produced closest to them in phase space. With 110,000 fully reconstructed D mesons from experiment E791 at Fermilab, the correlations are studied as functions of the $D\pi - D$ mass difference and of Feynman x. We observe significant correlations which appear to originate from a combination of sources including fragmentation dynamics, resonant decays, and charge of the beam.

While the production of heavy quarks can be calculated in perturbative Quantum Chromodynamics (QCD), the evolution of these quarks into hadrons remains one of the most challenging aspects of nonperturbative QCD. Correlations between charm mesons and the charged pions produced closest to them in phase space provide information on how quarks evolve into hadrons. Fragmentation dynamics [1], resonances [2], and beam effects can each produce such correlations. The relative importance of these mechanisms must be determined from data.

During fragmentation, correlations could be produced because $\overline{q}q$ pairs from the vacuum are neutral. For example, if a c quark combines with a $\overline{d}$ from such a pair to form a D^+, the remaining d is close by in phase space and is likely to become part of the closest pion, which we call the "associated pion". Thus, $D^+\pi^-$ ($D^-\pi^+$) would be favored and $D^+\pi^+$ ($D^-\pi^-$) disfavored. Similarly, $D^0\pi^+$ ($\overline{D^0}\pi^-$) would be favored and $D^0\pi^-$ ($\overline{D^0}\pi^+$) disfavored. Resonances produce the same favored associations. D^{*+} decay associates a π^+ with a D^0 while D^{*-} decay associates a π^- with a $\overline{D^0}$. Qualitatively, D^{**} decays produce the same correlations.

The charge of the beam particle can also lead to charge correlations. Using a π^- beam can lead to the association of both charm mesons and anticharm mesons with negative pions, especially in the forward (beam) direction. Two distinct but related mechanisms can lead to this result. If the charm quark (antiquark) produced in a hard interaction coalesces with the antiquark (quark) from the beam particle to form the charm (anticharm) meson, the remaining quark (antiquark) from the beam can become part of a negative pion, but not part of a positive pion. If neither the quark nor the antiquark from the beam pion is used in making the charm meson, both are available to form negative pions but not positive pions.

By comparing the charge correlations of different species of charm mesons and antimesons with associated pions, and by studying them as functions of Feynman x (x_F) of the charm meson, one can hope to disentangle some of these processes. Evidence of such correlations between B mesons and associated light mesons, ascribed to resonances, has been observed in Z^0 decays at LEP by the OPAL collaboration [3]. In this letter, we report the first observation of fragmentation and beam-related

production correlations for charm mesons.

We use $D^0 \to K^-\pi^+$, $D^+ \to K^-\pi^+\pi^+$, and $D^{*+} \to D^0\pi^+$ signals (and their charge conjugate decays) from experiment E791 at Fermilab for this study. The data were recorded using a 500 GeV/c π^- beam interacting in five thin target foils (one platinum, four diamond) separated by gaps of about 1.4 cm. The detector, described elsewhere in more detail [4], is a large-acceptance, forward, two-magnet spectrometer. Its key components for this study include eight planes of multiwire proportional chambers, six planes of silicon microstrip detectors (SMD) before the target for beam tracking, a 17-plane SMD system and 35 drift chamber planes downstream of the target for track and vertex reconstruction, and two multicell threshold Čerenkov counters for charged particle identification.

During event reconstruction, all events with evidence of well-separated production and decay vertices were retained as charm decay candidates. For this study, we require the candidate charm decay vertex to be located well outside the target foils and to be at least $8\sigma_\Delta$ downstream of the primary vertex (where σ_Δ is the error in the measured longitudinal separation between the vertices $\approx 350\mu$m). The momentum vector of the candidate D must point back to the primary vertex with impact parameter less than 80μm. The momentum of the D transverse to the line joining the primary and secondary vertices must be less than 0.35 GeV/c. Each decay track must pass closer to the secondary vertex than to the primary vertex. Finally, the track assigned to be the kaon in the charm decay must have a signature in the Čerenkov counters consistent with the kaon hypothesis. The $D^{*\pm}$ candidates are found from the $D^0/\overline{D^0}$ samples by adding $\pi^\pm$ tracks and requiring that the mass difference $\Delta m = M(D\pi) - M(D)$ be consistent with the $D^* \to D\pi$ hypothesis. The final signal sizes are obtained by fitting the invariant mass spectra as Gaussian signals and linear backgrounds. For D^0, $\overline{D^0}$, D^+, D^-, D^{*+}, and D^{*-}, the fits yield 22587 ± 210, 24237 ± 216, 24569 ± 204, 29649 ± 238, 4997 ± 84 and 6048 ± 93 events, respectively. The r.m.s. mass resolutions, σ_D, used later in defining signal and background bands, are 13 MeV/c^2, 13 MeV/c^2, and 14 MeV/c^2 for D^0, D^+, and D^{*+}, respectively.

For each D found in an event, all tracks originating from the primary vertex

and producing a pion signature in the Čerenkov counters are combined with the D. Among these combinations, the pion that forms the smallest invariant mass difference (Δm_{min}) with the D decay products is selected as the associated pion.

We define the correlation parameter α as

$$\alpha(D) \equiv \frac{\sum N_i(D\pi^q) - \sum N_i(D\pi^{-q})}{\sum N_i(D\pi^q) + \sum N_i(D\pi^{-q})}, \tag{1}$$

where $q = +, -, -, +, -, +$ for $D = D^0$, $\overline{D^0}$, D^+, D^-, D^{*+}, and D^{*-}, respectively, and $\sum N_i(D\pi^q)$ denotes the number of charm mesons for which the selected pion has the charge q. In the absence of correlations α is zero, and in maximally correlated cases it is unity.

We first study the $D\pi$ correlations as functions of Δm_{min} for $\Delta m_{min} < 0.74$ GeV/c^2. The number of $D\pi$ signal combinations in each Δm_{min} bin is determined by subtracting from the Δm_{min} distribution for D candidates (mass within $\pm 2.5\ \sigma_D$ of the nominal D mass) the appropriately normalized Δm_{min} distribution for background events (mass between 3.0 σ_D and 5.5 σ_D from the nominal D mass). The correlation parameters for background-subtracted signals (before additional corrections) and background regions are listed in Table 1. The signal correlations differ significantly from the background correlations. We note that replacing the D candidate in an event with a D of the same species from another event, while keeping the rest of the event the same, produces correlations consistent with those of the background.

We use a Monte Carlo simulation of the experiment and the LUND event generator (PYTHIA 5.7/JETSET 7.3) [5] to model the effects of our apparatus and reconstruction. This simulation describes the geometry, resolution, noise, and efficiency of all detectors, as well as interactions and decays in the spectrometer. The detected D^*/D production ratio in the Monte Carlo matches our data well. As with real events, the associated pion for each reconstructed D meson is selected. By matching the selected pion's momentum vector with the momenta of all generated particles, we determine whether the selected pion track is a real track or a ghost (false) track. Selecting a ghost pion (not matched to any generated track) or a real pion not matched to the

true associated pion can cause smearing in Δm_{min} and dilution of the correlation. Selecting a pion with the same charge as the associated pion but with different momentum smears events in Δm_{min}. Selecting a pion with the opposite charge smears events in Δm_{min} and also dilutes the correlation.

To account for the effects of ghost tracks, smearing, dilution, and acceptance on the correlations as functions of Δm_{min}, we employ a matrix formalism. For the D^+, the observed number of $D^+\pi^\mp$ combinations $O_j^{+\mp}$ in the j^{th} bin of Δm_{min} can be written as

$$O_j^{+\mp} = \sum_i S_{ji}^{1\mp} A_i^{+\mp} N_i^{+\mp} + \sum_i S_{ji}^{2\mp} A_i^{+\pm} N_i^{+\pm} + G_j^{+\mp} O_j^{+\mp} \qquad (2)$$

where $N_i^{+\mp}$ denotes the true number of $D^+\pi^\mp$ events in the ith bin of Δm_{min}, $A_i^{+\mp}$ the acceptance probability, and $G_j^{+\mp}$ the ghost track rate for $D^+\pi^\mp$ combinations. The matrix $S^{1\mp}$ describes smearing in the absence of dilution while the matrix $S^{2\mp}$ describes smearing and dilution when the wrong sign pion is selected. The smearing matrices $S^{1\mp}$ and $S^{2\mp}$, the acceptance coefficients A^{+-} and A^{++}, and the ghost track rates G^{+-} and G^{++} are determined from the Monte Carlo. The coupled matrix equations in (2) are solved to obtain the true distributions N_i^{+-} and N_i^{++}. Corrected Δm_{min} distributions are shown in Figure 1. The corrected correlation parameters for D, $\alpha(D)$, for $\overline{D}$, $\alpha(\overline{D})$, and for the D and $\overline{D}$ combined, $\alpha(D,\overline{D})$ are presented in column 4 of Table 1.

The statistical and systematic errors assigned to the final measurements, shown first and second respectively, are also given in Table 1. These errors are propagated through the matrix formalism. The systematic errors account for uncertainties in the Monte Carlo simulation of the detector (their effects on dilution, smearing, ghost tracks, and acceptance), analysis cuts, background subtraction, kaon misidentification, and binning (in decreasing order of importance as listed). For each data point, the systematic uncertainties due to these sources are added in quadrature. The systematic uncertainties due to statistical fluctuations in the Monte Carlo are negligible.

To verify the results produced by the matrix formalism, we also estimate the correlations using simple dilution factors (summed over all bins of Δm_{min}). For D^+, the true number of combinations, N_t^{+-} and N_t^{++}, can be expressed in terms of the

reconstructed combinations N_r^{+-} and N_r^{++} as

$$N_r^{+\mp} = (1 - d_{+\mp})N_t^{+\mp} + d_{+\pm}N_t^{+\pm}, \tag{3}$$

where the dilution factor $d_{+\mp}$ denotes the probability that a true $D^+\pi^\mp$ combination is reconstructed as a $D^+\pi^\pm$. The results from this technique are consistent with those reported in Table 1.

All studies and corrections have been done within the framework of the LUND PYTHIA/JETSET model. The dilution factors d_{ab} in Eq. (3) are typically of order $0.2 - 0.3$. In our Monte Carlo, $d_{+-} \approx d_{++}$ but d_{-+} is less than d_{--}. The difference between d_{--} and d_{-+} is almost independent of x_F with a typical value near 0.06. Varying some of the JETSET fragmentation parameters to reproduce our inclusive D^+/D^- production asymmetries as a function of x_F, as described in ref. [6], leads to results consistent with those in Table 1. A fundamentally different model of hadron production might change the differences between the d's discussed above by a few times 0.01, which would in turn change the measured correlation parameters. For example, reducing $(d_{--} - d_{-+})$ from 0.06 to 0.05 would increase $\alpha(D^-)$ by 0.02 – 0.03.

In Figs. 1(a) and (b) we present the numbers of $D^0\pi^\pm$ and $\overline{D^0}\pi^\mp$ combinations as functions of Δm_{min}. In both of these plots the combinations differ mainly in the $D^{*\pm}$ resonance region ,the first 75MeV/c^2 bin. Using a $\pm 2.5\sigma$ cut on the $D^{*+} - D^0$ and $D^{*-} - \overline{D^0}$ mass difference, we separate the final $D^0\pi^+$ and $\overline{D^0}\pi^-$ samples into resonance (res) and continuum ($cont$) contributions to obtain $\alpha(D^0_{res}) = 0.98 \pm 0.04$ and $\alpha(\overline{D^0}_{res}) = 0.98 \pm 0.02$. For pure resonance, α would be near 1. The measured values serve as a check of our method. The continuum measurements are $\alpha(D^0_{cont}) = -0.07 \pm 0.03$ and $\alpha(\overline{D^0}_{cont}) = 0.17 \pm 0.03$. In Figs. 1(c) and (d) we present the $D^+\pi^\mp$ and $D^-\pi^\pm$ combinations. In both these plots the combinations differ over a broad range in Δm_{min}. In Figs. 1(e) and (f) we present the $D^{*+}\pi^\mp$ and $D^{*-}\pi^\pm$ combinations. A pattern similar to that for $D^\pm$ is manifest. The plots for charm mesons and anticharm mesons clearly differ. These differences also appear in column (4) of Table 1, and indicate the presence of significant beam-related effects.

To investigate beam-related effects in more detail, we study the x_F dependence of

the D^+ and D^{*+} correlations. We do not show the correlations for D^0's since many D^0's are decay products of either D^{*0} and D^{*+}, making interpretation difficult. In Fig. 2, we plot α as a function of x_F, for both particle and antiparticle for D^+ and D^{*+}. The distributions are corrected using the simple dilution factor technique. We observe that $\alpha(D^+)$ rises slightly with x_F but $\alpha(D^-)$ falls sharply to negative values for $x_F > 0.2$. In both cases, the D's are more likely to be associated with π^-'s at high x_F where beam effects seem to be important. There appears to be less dependence of α on x_F for the $D^{*\pm}$.

Further beam-related studies with Monte Carlo data suggest the correlation asymmetries cancel under neutral beam conditions and are in fact symmetric. This is effectively accomplished when the combined particle and antiparticle correlations are computed. In Table 1, we show the combined and symmetrized correlation parameters to be $\alpha(D^0, \overline{D^0}) = 0.29 \pm 0.02 \pm 0.03$, $\alpha(D^+, D^-) = 0.21 \pm 0.02 \pm 0.03$, and $\alpha(D^{*+}, D^{*-}) = 0.23 \pm 0.04 \pm 0.03$. These results indicate that fragmentation dynamics and resonant decays produce substantial correlations between D mesons and their associated pions. All three combined correlation levels are approximately equal, although the correlations for neutral and charged D mesons are dominated by resonant and continuum regions of Δm_{min}, respectively.

In summary, we observe significant production correlations between D mesons and their associated pions. Some of these correlations are associated with fragmentation dynamics, some with resonances, and some with the charge of the beam. In addition to providing information on how heavy quarks evolve into hadrons, such correlations may provide tools for tagging flavor in *CP* violation studies in heavy flavor systems.

We gratefully acknowledge the staffs of Fermilab and of all the participating institutions. This research was supported by the Brazilian Conselho Nacional de Desenvolvimento Científico e Technológio, the Mexican Consejo Nacional de Ciencia y Tecnologica, the Israeli Academy of Sciences and Humanities, the U.S. Department of Energy, the U.S.-Israeli Binational Science Foundation and the U.S. National Science Foundation. Fermilab is operated by the Universities Research Association, Inc., under contract with the United States Department of Energy.

REFERENCES

[1] M. Gronau and J. L. Rosner, Phys. Rev. D 49 (1994) 254.

[2] M. Gronau, A. Nippe, and J. L. Rosner, Phys. Rev. D 47 (1992) 1988.

[3] OPAL Collaboration, R. Akers et al., Z. Phys. C66 (1995) 19.

[4] J. A. Appel, Ann. Rev. Nucl. Part. Sci. 42 (1992) 367; D. J. Summers et al., Proceedings of the XXVII$^{\rm th}$ Rencontre de Moriond, Electroweak Interactions and Unified Theories, Les Arcs, France, (15–22 March 1992) 417; S. Amato et al., Nucl. Instr. Meth. A 324 (1993) 535; S. Bracker et al., IEEE Trans. Nucl. Sci. 43 (1996) 2457.

[5] T. Sjöstrand, Comput. Phys. Commun. 82 (1994) 74.

[6] E791 Collaboration, E. M. Aitala et al., Phys. Lett. B 371 (1996) 157.

TABLES

TABLE I. The x_F- and Δm_{min}-integrated correlation parameters α defined in Eq. (1) for the background-subtracted signals prior to correction, for the corresponding backgrounds, and for the signals after correction using the matrix technique based on Eq. (2). $\alpha(D^0)$ and $\alpha(\overline{D^0})$ contain both D^* resonance and nonresonance contributions.

Charm	Signal α	Background α	Corrected Signal α
D^0	0.13 ± 0.01	-0.04 ± 0.01	$0.12 \pm 0.03 \pm 0.04$
$\overline{D}^0$	0.18 ± 0.01	0.04 ± 0.01	$0.42 \pm 0.02 \pm 0.03$
$D^0, \overline{D}^0$	0.16 ± 0.01	0.00 ± 0.01	$0.29 \pm 0.02 \pm 0.03$
D^+	0.18 ± 0.01	0.10 ± 0.01	$0.45 \pm 0.03 \pm 0.03$
D^-	0.08 ± 0.01	0.02 ± 0.01	$0.03 \pm 0.03 \pm 0.04$
D^+, D^-	0.13 ± 0.01	0.05 ± 0.01	$0.21 \pm 0.02 \pm 0.03$
D^{*+}	0.15 ± 0.02	0.08 ± 0.03	$0.33 \pm 0.05 \pm 0.03$
D^{*-}	0.08 ± 0.02	0.02 ± 0.03	$0.15 \pm 0.05 \pm 0.04$
D^{*+}, D^{*-}	0.12 ± 0.01	0.05 ± 0.02	$0.23 \pm 0.04 \pm 0.03$

FIGURES

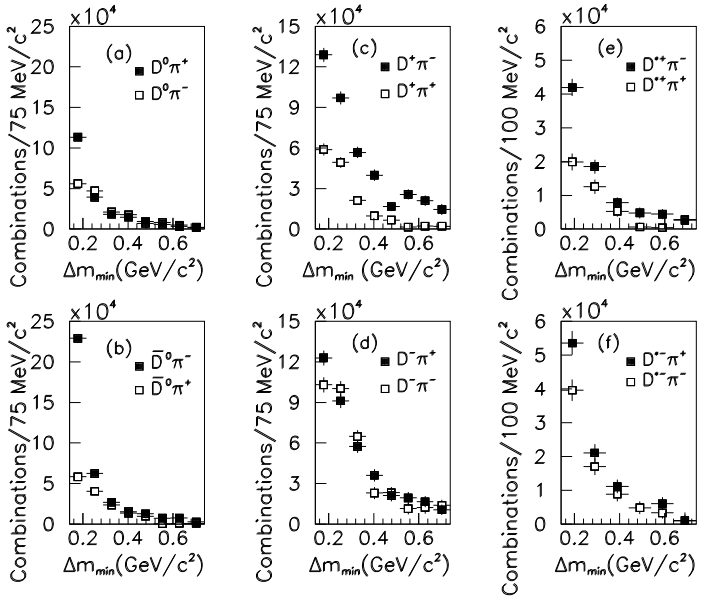

FIG. 1. The fully corrected Δm_{min} distributions for (a)$D^0\pi^{\pm}$, (b)$\overline{D^0}\pi^{\mp}$, (c)$D^+\pi^{\mp}$, (d)$D^-\pi^{\pm}$, (e)$D^{*+}\pi^{\mp}$, and (f)$D^{*-}\pi^{\pm}$ combinations. The error bars are statistical only.

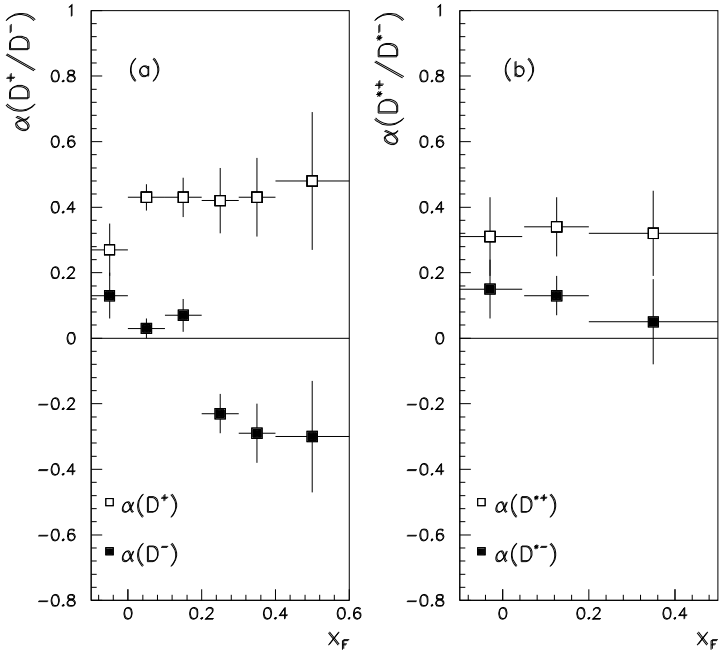

FIG. 2. The corrected correlation parameter α as a function of x_F for (a)D^+ and (b)D^{*+}. The parameter α is defined in Eq. (1) in the text. The error bars correspond to the statistical and systematic uncertainties added in quadrature. Additional model-dependence is discussed in the text.